Available online at: https://journal.upgripnk.ac.id/index.php/saintek
Jurnal Pendidikan Informatika dan Sains
15(1), 2026, 63-76
E-ISSN: 2407-1536
P-ISSN: 2089-2802

DESIGN AND EXPERIMENTAL PERFORMANCE ANALYSIS OF A DC MOTOR–AXIAL FLUX PERMANENT MAGNET GENERATOR (M-G) SYSTEM

Wiwit Indah Rahayu[1], Muhammad Ridhwan Sufandi[2]*, Hasan[2]
[1]Study Program of Electrical Engineering, Department of Electrical Engineering, Pontianak State Polytechnic, Pontianak, Indonesia
[2]Study Program of Electronic Systems Engineering Technology, Department of Electrical Engineering, Pontianak State Polytechnic, Pontianak, Indonesia
*email: mr.sufandi86@gmail.com

Received: 2026-03-04 Accepted: 2026-06-10 Published: 2026-06-30

Abstract
Renewable energy systems require reliable electrical generators to convert mechanical energy into electrical energy through the principle of electromagnetic induction. Among various generator technologies, the axial flux permanent magnet generator (AFPMG) has attracted considerable attention because of its compact structure, high efficiency, high power density, and excellent performance at low rotational speeds, making it suitable for small- and medium-scale renewable energy applications. However, the electrical performance of AFPMGs is strongly influenced by their design parameters and operating conditions, requiring experimental evaluation under controlled conditions. This study aims to design, fabricate, and experimentally evaluate a DC motor-driven axial flux permanent magnet generator (AFPMG) system for electromechanical DC–AC energy conversion. A DC motor was employed as the prime mover to drive the AFPMG, while the effects of stator winding turns, winding wire diameter, and permanent magnet dimensions on generator performance were investigated experimentally. Performance evaluation was conducted by measuring the output voltage, current, rotational speed, generated power, and overall electromechanical conversion efficiency of the integrated motor–generator system. The developed motor–generator system successfully generated stable alternating current (AC) output under various operating conditions. The experimental results demonstrate that the generator performance is significantly affected by the stator winding configuration and magnetic field strength, with improvements in these parameters leading to higher output voltage and power generation capability. The findings provide valuable insights into the design and optimization of compact axial flux permanent magnet generators for renewable energy applications.
Keywords: Axial Flux Permanent Magnet Generator, Motor–Generator System, Electromechanical Energy Conversion, Renewable Energy, Permanent Magnet.

How to cite (in APA style): Rahayu, W. I., Sufandi, M. R., & Hasan, H. (2026). Design and experimental performance analysis of a DC motor–axial flux permanent magnet generator (M-G) system. Jurnal Pendidikan Informatika Dan Sains, 15(1), 63–76. https://doi.org/10.31571/saintek.v15i1.10647

DOI: 10.31571/saintek.v15i1.10647

INTRODUCTION

Electrical energy has become an essential requirement in modern society, with global electricity demand continuing to increase due to industrial development and technological advancement. Although most electricity is still generated from conventional sources such as steam, thermal, and nuclear power plants, renewable energy resources including solar, wind, and hydropower have gained significant attention because of their sustainability and lower environmental impact. In renewable energy systems, mechanical energy obtained from natural resources is converted into electrical energy through electric generators based on the principle of electromagnetic induction. According to Faraday's law, an electromotive force (EMF) is induced when a conductor experiences a changing magnetic flux. Therefore, the performance of a generator depends on several factors, including rotor speed, magnetic field strength, and the effectiveness of the excitation system, all of which influence voltage stability and power generation capability (Farhan et al., 2021; Bianchi et al., 2018; Boldea & Nasar, 2020; Khan et al., 2019).

In laboratory-scale investigations and prototype development of renewable energy systems, a motor–generator (M–G) configuration is widely employed to evaluate generator performance under controlled operating conditions. In this electromechanical energy conversion system, electrical energy supplied to a DC motor is first converted into mechanical rotational energy. The rotating shaft of the DC motor subsequently drives an alternating current (AC) generator, which converts the mechanical energy into AC electrical energy through electromagnetic induction. This approach provides a stable and controllable prime mover, allowing the electrical characteristics of the generator, including output voltage, current, frequency, and power, to be experimentally evaluated over a range of operating conditions. Consequently, motor–generator systems have become an effective platform for studying generator performance and validating renewable energy technologies.

Among various generator technologies, the axial flux permanent magnet generator (AFPMG) has attracted considerable attention because of its compact structure, high power density, and superior efficiency compared with many conventional radial-flux generators. The AFPMG utilizes high-strength permanent magnets, such as Neodymium Iron Boron (NdFeB), to produce a strong magnetic field without requiring an external excitation current, thereby reducing electrical losses and improving overall efficiency. In addition, its axial magnetic flux configuration enables a lightweight and compact construction while maintaining excellent performance at relatively low rotational speeds. These characteristics make AFPMGs particularly suitable for small- and medium-scale renewable energy applications, including wind turbines, pico-hydropower systems, and other distributed generation systems where compact dimensions, high efficiency, and reliable operation are required (Ortiz-Garcia et al., 2024; Adi Suryantara et al., 2024; Xuan & Trong, 2025; Ferreira & Costa, 2024).

Despite these advantages, the electrical performance of an AFPMG is strongly influenced by its operating conditions, particularly rotational speed and loading. Variations in these parameters directly affect the generated voltage, output current, frequency, and overall power generation capability. Therefore, experimental evaluation using a controlled motor–generator system is necessary to accurately characterize the performance of the AFPMG under different operating conditions. Such investigations provide valuable information for optimizing generator design and assessing its suitability for renewable energy applications. Accordingly, this study aims to design, fabricate, and experimentally evaluate a DC motor-driven axial flux permanent magnet generator (AFPMG) system. The proposed motor–generator system employs a DC motor as the prime mover to rotate the AFPMG, enabling comprehensive performance evaluation based on output voltage, current, rotational speed, generated power, and overall electromechanical conversion efficiency. The findings are expected to contribute to the development of compact, efficient, and reliable electromechanical energy conversion systems for renewable energy applications.

METHOD

The research was conducted through three main stages: observation and system design, fabrication and assembly, and experimental performance evaluation. During the observation and system design stage, the main components of the motor–generator system were identified and analyzed. These components included the axial flux permanent magnet generator (AFPMG), the DC motor used as the prime mover, the coupling mechanism, the measuring instruments, and supporting electrical components. Particular attention was given to understanding the operating principle of the AFPMG, including electromagnetic induction, permanent magnet excitation, stator winding configuration, and the influence of rotational speed on the generated electrical output. Based on this analysis, the overall motor–generator system was designed to ensure reliable mechanical coupling and stable operating conditions during experimental testing.

The fabrication and assembly stage involved constructing the AFPMG and integrating it with the DC motor according to the proposed design. The generator rotor was equipped with permanent magnets, while the stator was fabricated using three-phase windings with predetermined numbers of turns and wire diameters. The completed AFPMG was mechanically coupled to the DC motor to establish a motor–generator (M–G) system capable of converting electrical energy supplied to the DC motor into mechanical rotational energy, which subsequently drove the generator to produce alternating current (AC) electrical output. Measuring instruments, including voltage, current, rotational speed, and power meters, were installed to monitor the operating characteristics of the system during testing.

The experimental performance evaluation was conducted by operating the motor–generator system under various generator winding configurations and rotational speeds. Performance measurements included output voltage, output current, rotational speed, output power, and overall system efficiency. Since the electrical input power was supplied to the DC motor rather than directly to the generator, the calculated efficiency represents the overall electromechanical efficiency of the integrated motor–generator system, including the mechanical losses associated with the motor and coupling mechanism. The experimental results were subsequently analyzed to evaluate the influence of winding parameters and operating conditions on the electrical performance of the AFPMG, including voltage characteristics, power generation capability, and system stability under different loading conditions. The experimental performance evaluation was conducted by operating the motor–generator system under various generator winding configurations and rotational speeds. Performance measurements included output voltage, output current, rotational speed, output power, and overall system efficiency. The experimental results were subsequently analyzed to evaluate the influence of winding parameters and operating conditions on the electrical performance of the AFPMG, including voltage characteristics, power generation capability, and system stability under different loading conditions.

The efficiency reported in this study represents the overall efficiency of the integrated motor–generator system. The input power corresponds to the electrical power supplied to the DC motor, while the output power corresponds to the electrical power generated by the AFPMG. Therefore, the calculated efficiency includes the electrical and mechanical losses of both the DC motor and the generator and should not be interpreted as the intrinsic efficiency of the AFPMG alone.

Power and Efficiency Measurement

The system is energized by applying voltage to the Axial Flux Permanent Magnet Generator circuit to establish a measurable current flow. The output power of the generator was determined using the AC power equation given in Equation (1).

$$P_{out} = I_{AC} \times V_{AC} \times cos\emptyset \quad (1)$$

where V_{AC} is the output voltage, I_{AC} is the output current, and $cos\ \emptyset$ is the load power factor. Since the experimental measurements were conducted using a resistive load, the power factor was assumed to be approximately one ($cos\ \emptyset\ \approx\ 1$). Consequently, the output power was calculated using Equation (2), as

$$P_{out} = I_{AC} \times V_{AC} \quad (2)$$

P = Power (watt)
I = Current (Ampere)
V = Voltage (Volt)
With the input power (Pin) and output power (Pout) values determined, the operational efficiency (η) of the Axial Flux Permanent Magnet Generator is calculated using the subsequent relationship shown in Equation (3).

$$Efficiency\ (\eta) = \frac{Output\ Power}{Input\ Power} \times 100\% \quad (3)$$

The fundamental principle governing the operation of three-phase AC machines is the creation of a rotating magnetic field within the stator. This is accomplished by applying a three-phase sinusoidal current to the spatially distributed stator windings, which generates a resultant magnetic flux vector that rotates continuously around the interior of the motor at synchronous speed, as expressed in Equation (4) (Kothari & Nagrath, 2017).

$$p = \left(\frac{120 \times f}{N_s}\right) \quad (4)$$

P = number of rotor poles
f = frequency (Hz)
N_s = The synchronous speed of the motor in revolutions per minute (rpm).

The rotor component is fabricated from transparent acrylic, configured as a circular disc with a 5 mm thickness. The determination of the magnet area is carried out using the subsequent formula shown in Equation (5).

$$A_{mg} = \pi \cdot r^2 \quad (5)$$

A_{mg} = magnetic cross-sectional area.
r = radius of the magnetic core

The theoretical expression for magnetic flux is derived from Faraday's law and the fundamental relation Φ=BA, where B is the magnetic flux density and A is the magnetic cross-sectional area. In practical magnetic circuit and transformer design, additional factors are often incorporated to account for the effects of multiple magnetic paths, leakage, fringing, and magnetic reluctance. Consequently, the maximum magnetic flux can be expressed in an extended empirical form as shown in Equation (6).

$$\Phi = A_{mg} \times B_{mg} \times m \times R \quad (6)$$

Φ = maximum magnetic flux (Weber, Wb)
A_{mg} = magnetic cross-sectional area (m^2)
B_{mg} = maximum magnetic flux density (Tesla, T)
m = number of magnetic paths or phases (dimensionless)
R = magnetic reluctance or correction factor (depending on the context of the equation)

RESULTS AND DISCUSSION

Design of Tools

To develop an efficient electromechanical energy conversion system, this research focuses on the design and fabrication of a DC motor-driven axial flux permanent magnet generator (AFPMG) system. The proposed motor–generator system employs a DC motor as the prime mover to drive the AFPMG, enabling the conversion of electrical energy supplied to the DC motor into mechanical rotational energy, which is subsequently converted into alternating current (AC) electrical energy by the generator through electromagnetic induction. The design of the AFPMG, including the stator winding configuration, permanent magnet arrangement, and mechanical assembly, plays an important role in determining the output voltage, power generation capability, and overall performance of the integrated motor–generator system. The design configuration of the proposed motor–generator system is illustrated in Figure 1.

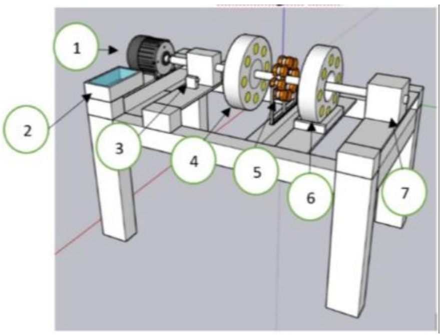

Figure 1. Design of DC to AC converter with permanent magnet axial flux type generator

Image Description: (1) DC Motor, (2) Panel Box, (3) RPM Optocoupler Sensor, (4) Rotor Disc and Neodymium Iron Boron (NdFeB) Magnet, (5) Wire Winding, (6) Stator Disc and Neodymium Iron Boron (NdFeB) Magnet, (7) UCP Pillow Block Shaft

Tool Assembly

The assembly of the proposed motor–generator system was carried out through several stages. First, the base frame was assembled to provide structural support for the entire system, followed by the installation of UCP pillow block bearings to support the generator shaft and ensure stable rotor rotation. A DC motor was then mounted on the frame and mechanically aligned with the generator shaft to serve as the prime mover. Next, the rotor was assembled by uniformly mounting Neodymium Iron Boron (NdFeB) permanent magnets on the rotor disc according to the predetermined pole configuration, ensuring correct magnetic polarity and equal spacing to produce a uniform magnetic field, as illustrated in Figure 2. The completed rotor was subsequently installed on the generator shaft and mechanically coupled to the DC motor.

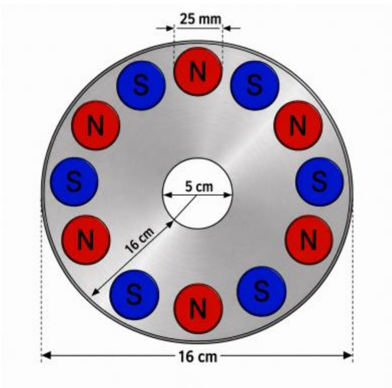

Figure 2. Rotor geometry and permanent magnet arrangement of the axial flux permanent magnet generator (AFPMG).

The stator was fabricated by winding enamel-coated copper wire according to the specified number of turns and wire diameter, after which it was mounted parallel to the rotor while maintaining an appropriate air gap to maximize electromagnetic induction without physical contact during operation. An optocoupler-based rotational speed (RPM) sensor was installed adjacent to the rotor and calibrated to ensure accurate rotational speed measurements throughout the experimental testing. Finally, the electrical measurement and control system was installed inside the control panel, consisting of the DC power supply, voltage and current measuring instruments, RPM monitoring unit, and other supporting electrical components. All electrical connections between the DC motor, the axial flux permanent magnet generator (AFPMG), the measuring instruments, and the load were completed according to the experimental design to ensure safe, stable, and reliable operation during performance evaluation.

Wiring Diagrams

The wiring diagram shows an electronic circuit involving several main components, namely the Hi-Link module as a power supply, Arduino Nano microcontroller, FC-03 series sensor, LCD screen and relay module can be seen in Figure 3.

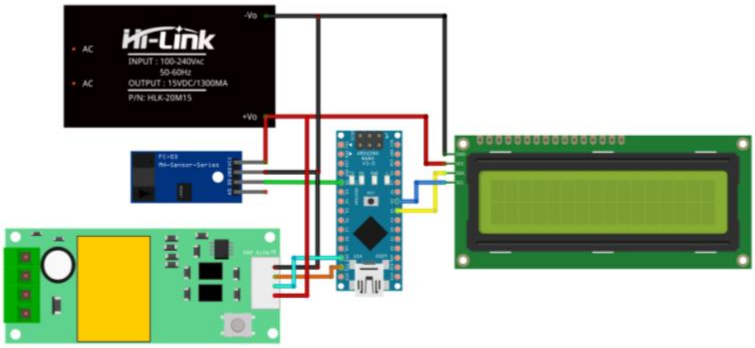

Figure 3. Wiring diagrams system

The electrical measurement and monitoring system was designed to support the experimental evaluation of the motor–generator system. An AC–DC power supply module (100–240 V AC input, 15 V DC/1300 mA output) was used to provide a stable DC voltage for the Arduino Nano, sensors, and other electronic components. The Arduino Nano functioned as the main controller by acquiring sensor signals, processing the measurement data, and displaying the results on the LCD module. The voltage, current, and rotational speed sensors were connected to the Arduino through the appropriate analog and digital input pins, enabling real-time monitoring of the operating parameters of the axial flux permanent magnet generator (AFPMG). The LCD module was interfaced with the Arduino to display the measured electrical quantities, while manual push buttons were provided for system initialization and operational control during the experimental tests. All components were integrated through the control panel to ensure reliable data acquisition and stable operation throughout the performance evaluation of the motor–generator system.

System Block Diagram

This block diagram illustrates the process flow of an Arduino Nano-based system involving several sensors as inputs, a microcontroller as a processor, and an LCD display as output. The block diagram shows how the system works by utilizing sensors for data collection, processing using a microcontroller, and displaying the results on an LCD screen, as illustrated in Figure 4.

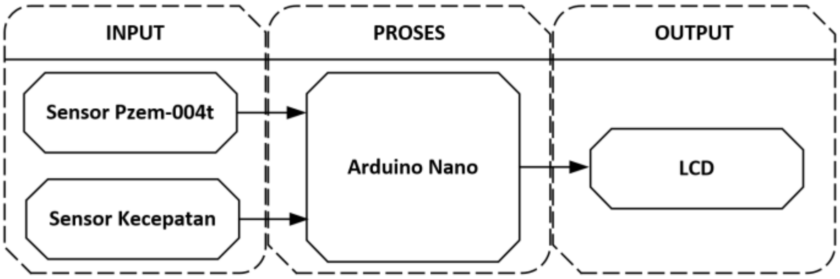

Figure 4. Wiring Diagram of Monitoring System Control

The PZEM-004T sensor measures electrical parameters such as voltage, current, power, and energy in an electrical circuit. The data generated by this sensor is sent to the Arduino for further processing. Meanwhile, the speed sensor detects or measures the speed of an object or machine. This data is also sent to the Arduino Nano for processing. The Arduino Nano functions as a data processing center. Data received from both sensors (the PZEM-004T and the speed sensor) is processed by the Arduino Nano. The Arduino then determines the output to be displayed on the LCD screen based on the processed data. The results of the Arduino Nano's processing are displayed on the LCD. This output includes information from the PZEM-004T sensor (such as voltage, current, power) and the speed sensor.

System Monitoring Control Flowchart

The flowchart in Figure 5 delineates the operational sequence of an automated monitoring system. The system, built upon an Arduino Nano microcontroller, integrates two primary sensors: the PZEM-004T and a dedicated speed sensor. A step-by-step breakdown of the process is provided below.

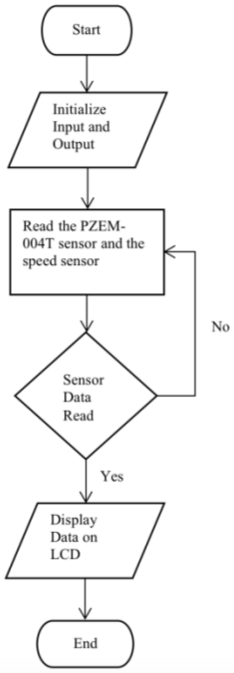

Figure 5. System monitoring control flowchart

The diagram outlines how the system autonomously acquires and processes data from these components : (1)System Initiation, the process commences upon system power-up. All components are prepared for initialization at this stage, (2) input/output initialization, the system initializes the sensors and the Liquid Crystal Display (LCD) then Arduino Nano configures communication with the PZEM-004T and speed sensors and sets up the LCD to serve as a data output display, (3) sensor data acquisition, the Arduino Nano proceeds to acquire data from both the PZEM-004T (which measures electrical parameters such as voltage, current, and power) and the speed sensor. The acquired data is then validated to ensure correct readings. If the data is successfully read, the process advances. If an error in data acquisition occurs, the system re-attempts the reading until valid sensor data is obtained, (4) data display, once the sensor data is successfully acquired and validated, the Arduino Nano transmits the processed information to the LCD for real-time display. The information presented includes key values such as voltage, current, and speed, corresponding to the monitored parameters, (5) process conclusion, upon displaying the data, the current process cycle concludes. The system is then prepared to re-enter the data acquisition loop, enabling continuous monitoring and updating of the displayed information.

Testing Parameters and Specifications

This section details the parameters and specifications used during the system testing phase. The test was conducted with a stator winding of 100 turns using a 1mm diameter wire and a 1.4 V DC input voltage to the motor. The detailed specifications of the components are as follows: (1) stator windings have a wire diameter of 1 mm, (2) the stator is composed of 9 winding units, connected in a series configuration, (3) the motor operates at a speed of 500 rpm, (4)The rotor features 12 poles, with each pole generating a voltage of 2.5 V AC and wound with 100 turns, (5) the air gap between the stator and rotor is 1 cm, (6) Neodymium (N52) magnets are used, each with a diameter of 2.5 cm and a thickness of 0.5 cm, (7) the rotor is equipped with 9 pairs of permanent magnets, arranged in alternating North and South poles. The complete experimental setup used for testing is shown in Figure 6.

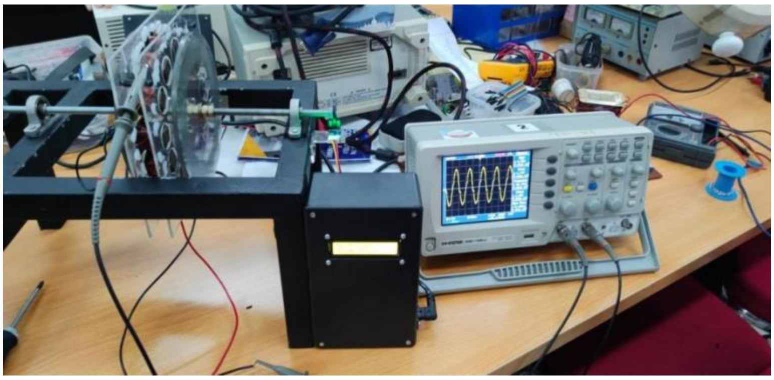

Figure 6. DC-to-AC Motor Generator System for a Permanent Magnet Axial Flux Generator

The experimental evaluation of the axial flux permanent magnet generator (AFPMG) was conducted using an oscilloscope to observe the induced voltage waveform generated by the stator windings during rotor rotation. This measurement approach is consistent with previous studies that employed laboratory-scale experimental setups to characterize the electromotive force (EMF) produced by axial flux permanent magnet generators under controlled operating conditions (Radwan-Pragłowska et al., 2020). The observed waveform provides direct evidence of the electromagnetic induction process and enables detailed evaluation of the generator's electrical output characteristics. During the experimental tests, the oscilloscope displayed a stable sinusoidal waveform, confirming that the AFPMG successfully generated alternating current (AC) electrical output. The characteristics of the generated waveform were influenced primarily by the rotational speed of the DC motor acting as the prime mover and the electromagnetic characteristics of the generator, including the stator winding configuration and permanent magnet arrangement. The oscilloscope measurements were used to verify the waveform quality and the stability of the generated AC output throughout the experimental evaluation.

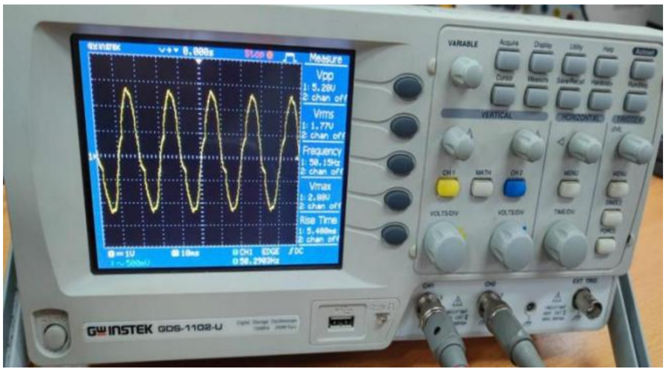

Figure 7. Experimental Results from Oscilloscope

Figure 7 illustrates that the voltage induced per winding is 2.5 V AC, while the total terminal voltage generated across all windings is 36 V AC at a fundamental frequency of 50 Hz.

Table 1. Output Power Measurement DC

Load (Watt)	Power Supply DC		
	Voltage DC (Volt)	Current DC (Ampere)	Power (Watt)
No Load	12	1.45	17.4
3 Watt	12	1.74	20.88
5 Watt	12	1.81	21.72
8 Watt	12	1.83	21.96
10 Watt	12	1.91	22.92
15 Watt	12	1.91	22.92

The data presented in Table 1 show the electrical input supplied by the DC power supply to the DC motor, which served as the prime mover for the motor–generator system. Throughout the experiments, the supply voltage was maintained at 12 V, while the input current increased from 1.45 A under no-load conditions to 1.91 A at 10 W and 15 W load conditions. Consequently, the electrical input power supplied to the DC motor increased from 17.4 W to 22.92 W as the generator load increased. The increase in motor input power indicates the additional mechanical power required to overcome the higher electromagnetic torque produced by the axial flux permanent magnet generator (AFPMG) under loaded operating conditions. The constant input power observed at the 10 W and 15 W load levels suggests that the motor–generator system had reached a stable operating region under the applied experimental conditions. These measurements represent the electrical input to the integrated motor–generator system rather than the input power of the AFPMG alone. Therefore, the values reported in Table 2 were used to determine the overall electromechanical conversion efficiency of the motor–generator system. This behavior is consistent with previous studies, which reported that increasing electrical load requires greater mechanical input power and influences the overall energy conversion performance of axial flux permanent magnet generators (Prasetijo, 2022; Rosa et al., 2023; Irasari & Widiyanto, 2023).

Table 2. Output Power Measurement AC

Axial Flux Permanent Magnet (AFPM) Generator				
Voltage AC (Volt)	Current AC (Ampere)	Power (Watt)	Frequency (Hz)	Angular Velocity (rpm)
247.7	0	0	50.2	505

Axial Flux Permanent Magnet (AFPM) Generator				
Voltage AC (Volt)	Current AC (Ampere)	Power (Watt)	Frequency (Hz)	Angular Velocity (rpm)
230.5	0.043	9.9115	49.8	504
227.7	0.046	10.4742	49.7	503
222.8	0.045	10.026	49.5	501
218	0.049	10.682	49.4	498
213.9	0.052	11.1228	49.4	498

The experimental data presented in Table 2 summarize the electrical output characteristics of the axial flux permanent magnet generator (AFPMG), including output voltage, output current, output power, output frequency, and rotational speed under different loading conditions. As the electrical load increased, the output current increased from 0 A under no-load conditions to 0.052 A at the maximum load, resulting in an increase in the generated output power from 0 W to 11.12 W. Meanwhile, the output voltage gradually decreased from 247.7 V to 213.9 V, accompanied by slight reductions in output frequency from 50.2 Hz to 49.4 Hz and rotational speed from 505 rpm to 498 rpm. These results indicate that increasing the electrical load required greater mechanical torque from the DC motor acting as the prime mover, thereby causing a slight decrease in rotational speed and consequently affecting the generated voltage and frequency.

When compared with the electrical input supplied to the DC motor (Table 2), the increase in generated output power was accompanied by an increase in the electrical input required to drive the motor. This behavior demonstrates the load-dependent characteristics of the integrated motor–generator system, where the electrical energy supplied to the DC motor was converted into mechanical rotational energy and subsequently into AC electrical energy by the AFPMG. The observed performance is consistent with previous studies, which reported that increasing electrical load leads to higher generated current and output power, accompanied by slight reductions in terminal voltage, rotational speed, and output frequency due to the increased electromagnetic torque acting on the generator (Eldoromi et al., 2018; Di Dio et al., 2022).

Table 4. Overall Electromechanical Conversion Efficiency of the Motor–Generator System

Load (Watt)	Power Supply DC Power (Watt)	AFGMr Power (Watt)	Efficiency (%)
No Load	17.4	0	0.00%
3 Watt	20.88	9.9115	47.41%
5 Watt	21.72	10.4742	48.22%
8 Watt	21.96	10.026	45.66%
10 Watt	22.92	10.682	46.61%
15 Watt	22.92	11.1228	48.53%

The efficiency values presented in Table 4 were calculated by comparing the electrical output power generated by the axial flux permanent magnet generator (AFPMG) with the electrical input power supplied to the DC motor, which served as the prime mover of the integrated motor–generator system. Therefore, the calculated efficiency represents the overall electromechanical conversion efficiency of the motor–generator system, rather than the intrinsic efficiency of the AFPMG alone, since the measured input power includes the electrical and mechanical losses associated with the DC motor, shaft coupling, and generator. The experimental results show that the overall system efficiency ranged from 45.66% to 48.53%, with an average efficiency of 47.28% under the investigated loading conditions. These results indicate that the energy conversion performance of the integrated motor–

generator system was influenced by the applied electrical load, mechanical transmission losses, and the electrical characteristics of the generator.

The observed load-dependent characteristics are consistent with previous studies on axial flux permanent magnet generators, which reported that generator topology, electromagnetic design, winding configuration, magnetic circuit optimization, and operating load significantly influence electrical output characteristics and overall electromechanical energy conversion performance. Systematic load variation testing is therefore essential for evaluating the operational capability and stability of axial flux permanent magnet generators under practical operating conditions (Vatani et al., 2025; Zhu et al., 2023; Kumar & Singh, 2024; Wang et al., 2023; Kurt et al., 2021; Yang et al., 2021; Ozdemir & Aydın, 2022; Li & Wang, 2023).

The experimental evaluation of the integrated motor–generator system was conducted under external load conditions ranging from no-load to 15 W while maintaining a constant 12 V DC supply to the DC motor. The experimental results show that the electrical input power supplied to the DC motor increased from 17.4 W under no-load conditions to 22.92 W at the 10 W and 15 W load levels. This increase indicates that greater electrical input was required by the DC motor to provide the additional mechanical torque needed to drive the axial flux permanent magnet generator (AFPMG) as the electrical load increased. The nearly constant input power observed at the 10 W and 15 W load conditions suggests that the motor–generator system reached a stable operating region under the applied experimental conditions.

The observed increase in motor input power with increasing electrical load reflects the typical load–response behavior of electromechanical energy conversion systems. As the generator supplied more electrical power to the load, the prime mover was required to deliver greater mechanical power to maintain generator operation. Similar behavior has been reported in previous studies on axial flux permanent magnet generators, where variations in loading conditions significantly influence the electrical output characteristics and the overall performance of motor–generator systems. These findings highlight the importance of systematic load testing for evaluating the operational characteristics and electromechanical energy conversion performance of AFPM generators under practical operating conditions (Saleh et al., 2021; Setyawan et al., 2022).

CONCLUSION

The developed motor–generator system employed an axial flux permanent magnet generator (AFPMG) equipped with nine pairs of Neodymium (N52) permanent magnets, each measuring 2.5 cm in diameter and 0.5 cm in thickness. The stator consisted of nine series-connected windings fabricated using 1 mm diameter copper wire. The AFPMG was driven by a 12 V DC motor acting as the prime mover and was experimentally evaluated under no-load and resistive load conditions of 3 W, 5 W, 8 W, 10 W, and 15 W.

The experimental results demonstrate that the proposed motor–generator system operated reliably under all tested loading conditions. As the electrical load increased, the output current increased from 0 A to 0.052 A, while the output voltage gradually decreased from 247.7 V to 213.9 V. Meanwhile, the rotational speed and output frequency remained relatively stable, decreasing only slightly from 505 rpm to 498 rpm and from 50.2 Hz to 49.4 Hz, respectively. These results indicate that the AFPMG maintained stable electrical performance despite variations in loading conditions.

The overall electromechanical conversion efficiency of the integrated motor–generator system ranged from 45.66% to 48.53%, with the highest efficiency obtained at the 15 W load condition and an average efficiency of approximately 47.28% across all loading conditions. It should be noted that this efficiency represents the overall performance of the integrated motor–generator system, including the electrical and mechanical losses of both the DC motor and the AFPMG, rather than the intrinsic efficiency of the generator alone. Overall, the proposed motor–generator system demonstrated stable operation and satisfactory electrical performance, indicating its potential for laboratory-scale evaluation and the development of compact renewable energy generation systems.

ACKNOWLEDGEMENT
The authors wish to express their deepest gratitude to Politeknik Negeri Pontianak for providing the necessary research facilities and institutional support that made this work possible. Special appreciation is extended to the Department of Electrical Engineering for their invaluable resources and supportive academic environment.

REFERENCES
Adi Suryantara, I. M., Indra Partha, C. G., & Sukerayasa, I. W. (2024). Rancang bangun generator magnet permanen fluks aksial pada prototype pembangkit listrik tenaga bayu (PLTB) sumbu vertikal. *Jurnal SPEKTRUM*, 11(1), 108–115. https://doi.org/10.24843/SPEKTRUM.2024.v11.i01.p12

Bianchi, F. D., De Battista, H., & Mantz, R. J. (2007). Wind turbine control systems: Principles, modelling and gain scheduling design. *Springer*. https://doi.org/10.1007/1-84628-493-7

Diaz, M., Rojas, A., & Rodríguez, J. (2025). Power electronics for energy transition and renewable energy conversion processes. *Processes*, 13(11), 3650. https://doi.org/10.3390/pr13113650

Di Dio, V., Cipriani, G., & Manno, D. (2022). Axial flux permanent magnet synchronous generators for pico hydropower application: A parametrical study. *Energies*, 15(19), 6893. https://doi.org/10.3390/en15196893

Duan, P., Liu, L. Y., Luo, X. L., Zhou, Y. Z., Tianyou, Y., & Yang, S. Y. (2025). Response-function framework for evaluating converter topologies in renewable energy integration. *Frontiers in Energy Research*, 13, Article 1734909. https://doi.org/10.3389/fenrg.2025.1734909

Eldoromi, M., Tohidi, S., Feyzi, M. R., Rostami, N., & Emadifar, R. (2018). Improved design of axial flux permanent magnet generator for small-scale wind turbine. *Turkish Journal of Electrical Engineering and Computer Sciences*, 26(6), 3084–3099. https://doi.org/10.3906/elk-1711-402

Farhan, M., Hidayat, R., & Saragih, Y. (2021). Pengaruh pembebanan terhadap arus eksitasi generator unit 2 PLTMH Curug. *Jurnal Simetrik*, 11(1), 398–403.

Ferreira, A. P., & Costa, A. F. (2024). Direct driven axial flux permanent magnet generator for small-scale wind power applications. *Renewable Energy and Power Quality Journal*, 9(1). https://doi.org/10.24084/repqj09.492

Hollweg, G. V., Singh Chawda, G., Chaturvedi, S., Bui, V.-H., & Su, W. (2025). Optimization techniques for low-level control of DC–AC converters in renewable-integrated microgrids. *Energies*, 18(6), 1429. https://doi.org/10.3390/en18061429

Irasari, P., & Widiyanto, P. (2023). Desain dan simulasi GMP fluks aksial berbasis dimensi magnet permanen komersil. *ELKOMIKA: Jurnal Teknik Energi Elektrik, Teknik Telekomunikasi, & Teknik Elektronika*. https://ejurnal.itenas.ac.id/index.php/elkomika/article/view/3650

Khair, M. R., Sofyan, A., Anugrah, A., & Anthony, Z. (2025). Perancangan generator magnet permanen tipe axial kecepatan rendah untuk pembangkit listrik tenaga angin skala kecil. *Kohesi: Jurnal Sains dan Teknologi*, 6(4), Article 9585. https://doi.org/10.3785/kohesi.v6i4.9585

Khan, M. J., Iqbal, M. T., Qu, P. Z., & Sopian, K. (2019). Renewable energy generation systems and control strategies. *Renewable Energy Focus*, 30, 12–22. https://doi.org/10.1016/j.ref.2019.08.001

Kothari, D. P., & Nagrath, I. J. (2017). Electric machines (5th ed.). McGraw Hill Education.

Kumar, P., & Singh, R. (2024). Performance analysis and optimization of axial flux machines for renewable energy applications. *Renewable Energy*, 202, 202–213. https://doi.org/10.1016/j.renene.2023.10.058

Kurt, E., Gor, H., & Celik, K. (2021). Optimization of a 3-kW axial flux permanent magnet generator with variable air gap. *International Transactions on Electrical Energy Systems*, 31(9), e13085. https://doi.org/10.1002/2050-7038.13085

Li, H., Wang, Z., & Blaabjerg, F. (2024). Advanced control techniques for DC–AC converters in renewable energy systems: A review. IEEE Transactions on Power Electronics, 39(4), 2735–2750. https://doi.org/10.1109/TPEL.2023.3333995

Ortiz-Garcia, E., Ramirez, J. M., & Dorrego-Portela, J. R. (2024). Design and performance evaluation of an axial flux permanent magnet generator for micro-wind applications. *International Journal of Power Systems*, 9, 17–25.

Ozdemir, M., & Aydın, F. (2022). Comparative performance analysis of axial flux permanent magnet generators under varying load conditions. *Journal of Renewable and Sustainable Energy*, 14(5), 053501. https://doi.org/10.1063/5.0093508

Prasetijo, H. (2022). Pengaruh inti stator terhadap performa generator magnet permanen fluks aksial satu fasa. *Jurnal Riset Sains dan Teknologi*, 6(2), 165–169. https://doi.org/10.30595/jrst.v6i2.13668

Radwan-Pragłowska, N., Wegiel, T., & Borkowski, D. (2020). Modeling of axial flux permanent magnet generators. *Energies*, 13(21), 5741. https://doi.org/10.3390/en13215741

Rosa, M. K. A., Jonrinaldi, & Sianipar, H. F. (2023). Rancang bangun generator fluks aksial magnet permanen satu fasa 12 kutub dengan stator ganda. *Jurnal Informatika dan Teknik Elektro Terapan*, 11(3s1). https://doi.org/10.23960/jitet.v11i3s1.3377

Saleh, Z., Apriani, Y., Karim, K., & Aldiansyah, A. (2021). Analysis of performance of permanent magnet generator fluks axial 1 phase with load variation. *Journal of Robotics and Control*, 2(2), 98–102. https://doi.org/10.18196/jrc.2260

Setyawan, E. Y., Soleh, C., Krismanto, A. U., Sujana, I. W., & Prihatmi, T. N. (2022). Design and performance analysis of double axial flux permanent magnet generator. *Trends in Sciences*, 19(6), Article 3049. https://doi.org/10.48048/tis.2022.3049

Simani, S., Alvisi, S., & Venturini, M. (2019). Data-driven control techniques for renewable energy conversion systems: Wind turbine and hydroelectric plants. Electronics, 8(2), Article 237. https://doi.org/10.3390/electronics8020237Singh, R., & Jain, S. (2023). Grid-connected renewable energy systems: Challenges and solutions for power quality and synchronization. *Renewable and Sustainable Energy Reviews*, 174, 113123. https://doi.org/10.1016/j.rser.2023.113123

Vu Xuan, H., & Nguyen Trong, V. (2025). Effective electromagnetic models for the design of axial flux permanent magnet generators in wind power. *Engineering Proceedings*, 104(1), 82. https://doi.org/10.3390/engproc2025104082

Vatani, M., Mohammadi, A., Lewis, D. D., Eastham, J. F., & Ionel, D. M. (2025). Axial flux permanent magnet generators for direct-drive wind turbines: Review and optimal design studies. *IEEE Transactions on Industry Applications*, 61(6), 9615–9627. https://doi.org/10.1109/TIA.2025.3521427

Wang, J., Zhao, Q., & Li, Z. (2023). Impact of load dynamics on electrical performance of low-speed permanent magnet generators. *Energy Conversion and Management*, 278, 116637. https://doi.org/10.1016/j.enconman.2023.116637

Wirtayasa, K., Kasim, M., Widiyanto, P., Muqorobin, A., Wijanarko, S., & Irasari, P. (2025). Permanent magnet generator performance comparison under different topologies and capacities. *International Journal of Power Electronics and Drive Systems*, 16(3), 1516–1527. https://doi.org/10.11591/ijpeds.v16.i3.pp1516-1527

Yang, X., Liu, J., & Huang, S. (2021). Investigation of an axial flux permanent magnet generator with concentrated windings for micro-wind applications. Sustainable Energy Technologies and Assessments, 45, 101175. https://doi.org/10.1016/j.seta.2020.101175

Zhu, L., Li, H., & Chen, Y. (2023). Efficiency enhancement techniques for axial flux permanent magnet machines under variable loading conditions. *IEEE Transactions on Industry Applications,* 59(4), 3018–3027. https://doi.org/10.1109/TIA.2023.3287625